Clustering as a Prerequisite for Chimera States in Globally Coupled Systems

Lennart Schmidt[1,2] and Katharina Krischer[1,*]
[1]Physik-Department, Nonequilibrium Chemical Physics, Technische Universität München, James-Franck-Str. 1, D-85748 Garching, Germany
[2]Institute for Advanced Study - Technische Universität München, Lichtenbergstr. 2a, D-85748 Garching, Germany
(Received 4 September 2014; published 22 January 2015)

The coexistence of coherently and incoherently oscillating parts in a system of identical oscillators with symmetrical coupling, i.e., a chimera state, is even observable with uniform global coupling. We address the question of the prerequisites for these states to occur in globally coupled systems. By analyzing two different types of chimera states found for nonlinear global coupling, we show that a clustering mechanism to split the ensemble into two groups is needed as a first step. In fact, the chimera states inherit properties from the cluster states in which they originate. Remarkably, they can exist in parameter space between cluster and chaotic states, as well as between cluster and synchronized states.

DOI: 10.1103/PhysRevLett.114.034101 PACS numbers: 05.45.-a

The story of chimeras in nonlinear dynamics goes back to the year 2002, when Kuramoto and Battogtokh [1] discovered that in a system of identical oscillators with symmetrical coupling, coherently oscillating regions can coexist with incoherent ones. In fact, this was not the first observation of such a coexistence [2–4], but Kuramoto and Battogtokh were the first pointing out its importance. This state was named a chimera state by Abrams and Strogatz [5], referring to the chimera in Greek mythology. Many theoretical studies followed, see, for example, Refs. [5–12], and 10 years after their discovery, chimera states could be observed in experiments also [13–18]. For a recent review, see Ref. [19]. Yet, concerning the prerequisites of their existence and the mechanisms of their emergence only very little is known. Bifurcation analysis revealed that they can emerge via a saddle-node bifurcation [5,7,9,20], and they were found in maps with coupling-induced bistability [10]. First analytical studies aiming to analyze the stability and to characterize the emergence and dynamics of chimera states in nonlocally coupled systems in a general way are presented in Refs. [20,21]. In addition, it has long been thought that a nonlocal coupling scheme is indispensable for their formation. Under nonlocal coupling, it is reasonable that regions of different dynamics can coexist, since the coupling decreases with the distance and the influence of one region on the other over some interfacial region might not be too strong. However, it could be shown that they also exist in systems with uniform global coupling [11,12,18,22], where each oscillator is influenced equally strongly by all the other oscillators. Such a coupling is realized experimentally, e.g., by an external resistance in series with some voltage-controlled device, such as a gas-discharge tube [23] or an electrochemical cell [24] or due to rapid mixing in the gas phase in surface reactions [25,26]. Generally, it arises whenever a global quantity is controlled and can be linear, as well as nonlinear. For globally coupled phase oscillators, chimera states were found in a system with time delay, where bistability emerged in a self-consistent way, as well as with individual bistable oscillators [11].

In this Letter, we argue that a clustering mechanism observed typically in globally coupled systems is a sufficient feature, rendering chimera states possible, as it splits the oscillators into several groups and yields at least bistability. Then, one of the two groups can desynchronize, while the other group stays coherent if the response on the coupling is effectively different in the two groups. In the present study, we demonstrate that this situation can arise via nonlinear amplitude effects. Moreover, we show that different cluster states lead to different chimera states and that the chimera states inherit properties from the cluster states in which they originate.

Our system is composed of N Stuart-Landau oscillators, each of the form

$$\frac{d}{dt}W_k = W_k - (1+ic_2)|W_k|^2 W_k, \tag{1}$$

$k = 1, 2, \ldots, N$, constituting generic limit-cycle oscillators near a Hopf bifurcation [27]. We couple them via a nonlinear global coupling:

$$\frac{d}{dt}W_k = W_k - (1+ic_2)|W_k|^2 W_k - (1+i\nu)\langle W\rangle + (1+ic_2)\langle |W|^2 W\rangle. \tag{2}$$

Here, $\langle\cdots\rangle$ describes the arithmetic mean of the oscillator population, i.e., $\langle W\rangle = \sum_{k=1}^{N} W_k/N$. Taking the average of the whole equation yields for the dynamics of the mean value

$$\frac{d}{dt}\langle W\rangle = -i\nu\langle W\rangle \Rightarrow \langle W\rangle = \eta e^{-i\nu t}. \quad (3)$$

This constitutes conserved harmonic oscillations of the ensemble average. Note that the above model, Eq. (2), describes the essential dynamics of the oxide-layer thickness during the photoelectrodissolution of n-type silicon [28–30]. The linear global coupling is a result of an external resistance in series with the silicon electrode, while we believe that the nonlinear global coupling is connected to a limitation of the total amount of charge carriers. For more details, see Refs. [30,31]. This experimental system exhibits also chimera states [18,31]. To capture its dynamics, it is important to reproduce the harmonic mean-field oscillation.

The dynamics of the oscillator population, Eq. (2), are determined by three parameters, namely c_2, ν, and η, where η is controlled via initial conditions and acts effectively as the coupling strength. We numerically solved Eq. (2) using an implicit Adams method with time step $dt = 0.01$ for $N = 1000$ oscillators and random initial conditions fulfilling the conservation law in Eq. (3). The simulation results reveal two types of clustering dynamics: amplitude clusters as depicted in Fig. 1(a) and modulated amplitude clusters as depicted in Fig. 1(f). In the amplitude cluster state, the ensemble splits into two groups that oscillate with an amplitude difference and a small, fixed phase difference. The modulated amplitude cluster state can be described as an overall uniform oscillation that is modulated by an additional oscillation of the two groups around the mean value in antiphase, giving rise to quasiperiodic motion. We studied these cluster solutions in detail in Ref. [32], where we could show that the amplitude clusters bifurcate off the synchronized solution [Fig. 1(c)] via a pitchfork bifurcation. The modulated amplitude clusters are created in a secondary Hopf bifurcation, and the two types of clusters are connected by a saddle-node of infinite period (SNIPER) bifurcation. The cluster formation is the first symmetry-breaking step rendering chimera states possible as it produces first of all two different groups. Indeed, in the vicinity of the two types of clusters, we also observe two associated types of chimera states, as shown in Figs. 1(b) and 1(e), respectively. The first type obviously inherited the property that the two groups are separated by an amplitude difference. Thus, starting from the amplitude cluster state, the group with the smaller radius got desynchronized. The second type of chimeras also shares properties with the modulated amplitude clusters, but this will be discussed below, where it becomes more apparent. Type II chimeras

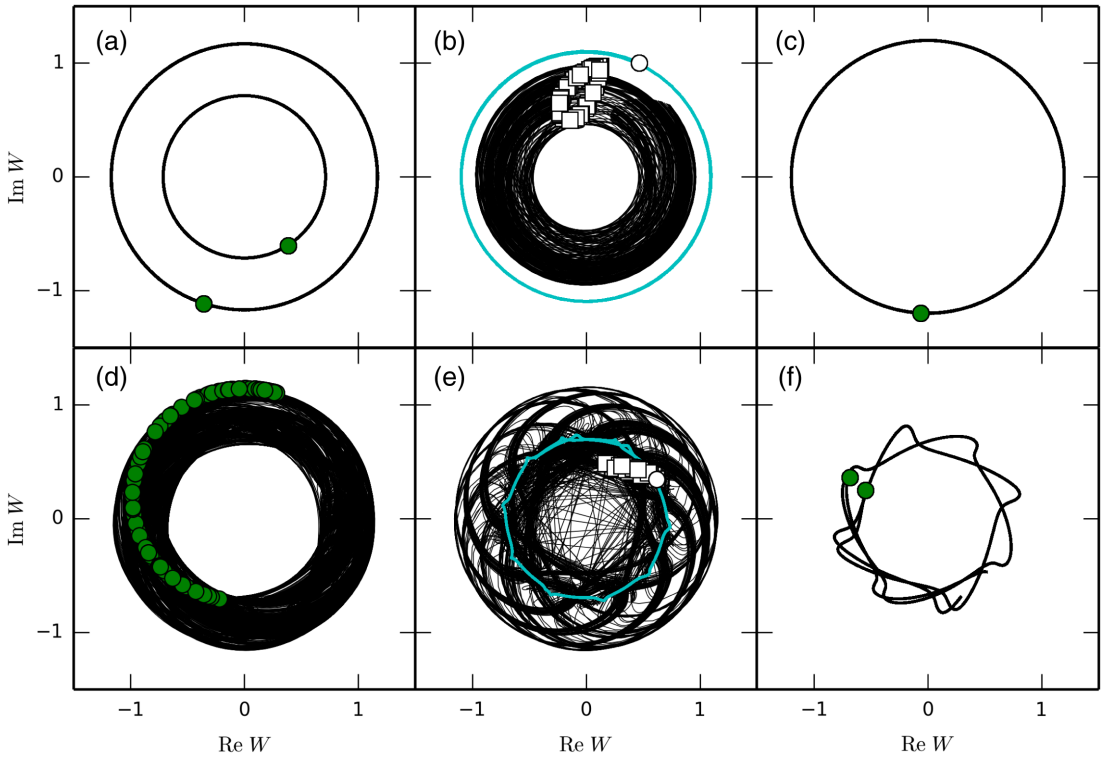

FIG. 1 (color online). Evolutions in the complex plane and snapshots. Trajectories of the oscillators are shown as solid lines, whereas the symbols describe snapshots of the system. First row: type I dynamics. (a) Amplitude clusters ($\eta = 0.9$). (b) Type I chimera ($\eta = 1.02$), black lines and squares: incoherent group; cyan (gray) lines and circles: coherent group. (c) Complete synchronization ($\eta = 1.2$). Other parameters: $c_2 = 0.58$ and $\nu = 1.49$. Second row: type II dynamics. (d) Irregular dynamics ($\nu = -0.1$). (e) Type II chimera ($\nu = 0.02$), black lines and squares: incoherent group; cyan (gray) lines and circles: coherent group. (f) Modulated amplitude clusters ($\nu = 0.1$). Other parameters: $c_2 = -0.6$, $\eta = 0.7$.

[Fig. 1(e)] could actually be identified with the chimera states found during the photoelectrodissolution of n-type silicon [18,30,31]. It bridges the gap between the cluster solution in Fig. 1(f) and completely irregular dynamics in Fig. 1(d). In contrast, type I chimeras mediate between the cluster solution in Fig. 1(a) and the synchronized state in Fig. 1(c). Phase diagrams in the vicinity of the two types of chimera states can be found in the Supplemental Material [33].

To gain a better understanding of the temporal dynamics in the chimera states, we depict $|W_k|$ and Re W_k versus time for type I and II chimeras in Figs. 2(a) and 2(c), respectively. The synchronized group is marked with cyan (gray) color and the incoherent group is plotted in black. In the type I chimera, there is a clear separation of the groups by an amplitude difference. This state is in fact unstable, as we observe heteroclinic transitions between the type I chimera and two other cluster states on a large time scale. This will be discussed below. In contrast, the second type of chimeras seems to be stable, as we could not observe a break down in the simulations up to $T = 1 \times 10^6$. The incoherent oscillators in this type II chimera show a nearly periodic spiking behavior (which is not performed by all incoherent oscillators at the same time). This is a property inherited from the modulated amplitude clusters [Fig. 1(f)]. The frequency of the spiking is given by the frequency of the modulational oscillations that are a result of a secondary Hopf bifurcation [32]. The dynamics show that the separations into incoherent and coherent groups occur via the clustering mechanism, for both types of chimeras.

Type I chimeras can also be found with a linear global coupling. Daido and Nakanishi [22] and also Nakagawa and Kuramoto [4] describe a state that seems to be such a chimera state, but they do not identify them as such. Only later, they have been identified as chimera states [12]. In fact, the nonlinear global coupling we consider behaves effectively like a linear global coupling in case of type I dynamics. This is visualized in Fig. 2(b), where we plot the linear part of the coupling $\langle W \rangle$ as a red dashed line and the nonlinear part $\langle |W|^2 W \rangle$ as a blue solid line. We see that the nonlinear term is also sinusoidal, i.e., $\langle |W|^2 W \rangle \propto \langle W \rangle$, yielding an effective overall linear behavior of the coupling. Since this implies $\langle |W_k|^2 W_k \rangle = \langle r_k^3 e^{i\phi_k} \rangle \propto \langle r_k e^{i\phi_k} \rangle$, averaging leads to vanishing nonlinear effects in the global coupling for type I chimeras. In contrast, in case of type II chimeras, the dynamics of $\langle |W|^2 W \rangle$ is highly nonlinear, as shown in Fig. 2(d). We conclude that type II dynamics might not be observable with a solely linear global coupling.

Furthermore, we looked at time series of individual oscillators in the incoherent groups. Examples are depicted in Figs. 3(a) and 3(c) for type I and II chimeras, respectively. As a simple test for chaoticity, next-maximum maps for the time series are shown in Figs. 3(b) and 3(d), respectively. Both next-maximum maps are highly nontrivial and structurally very different. We see this as a clear indication that the dynamics in the incoherent parts of the two types of chimeras take place on different types of chaotic attractors. In the case of type II chimeras, the incoherent dynamics inherits properties from the motion on the torus existing at close-by parameter values, while no torus exists in the neighborhood of type I chimeras.

As already mentioned, type I chimeras are unstable, and we observe heteroclinic connections. To visualize this, we

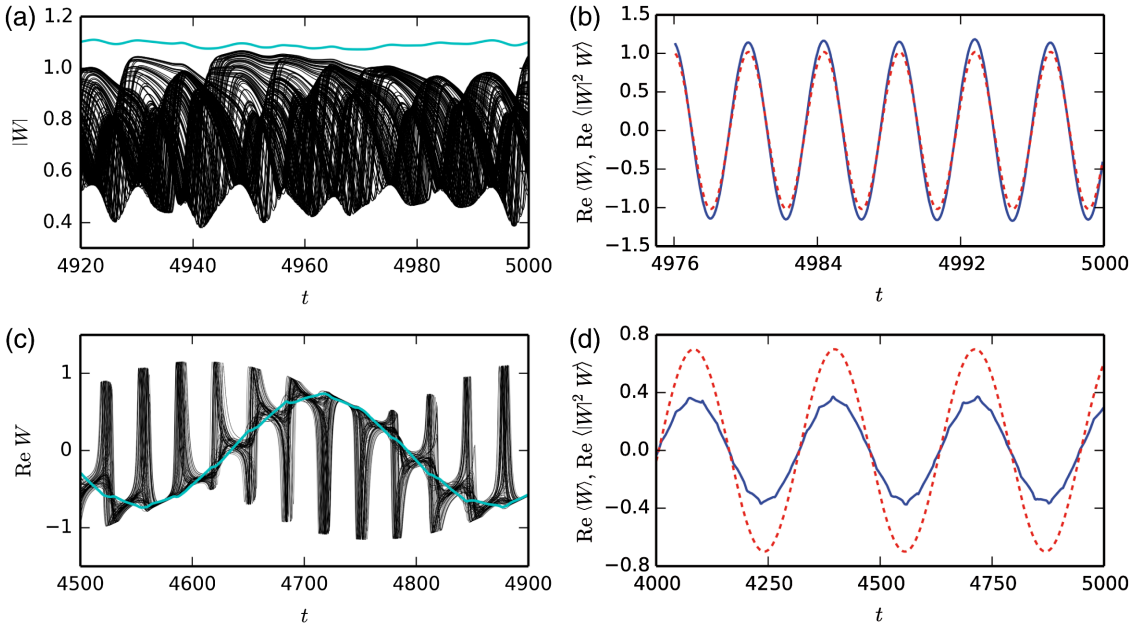

FIG. 2 (color online). (a),(c) Type I and II chimera states, modulus and real part versus time, respectively. The population splits into two groups, one being synchronized (cyan, gray) and one being desynchronized (black). (b),(d) Linear average, Re $\langle W \rangle$, (dashed lines) and nonlinear average, Re $\langle |W|^2 W \rangle$, (solid lines) versus time for type I chimeras (b) and type II chimeras (d).

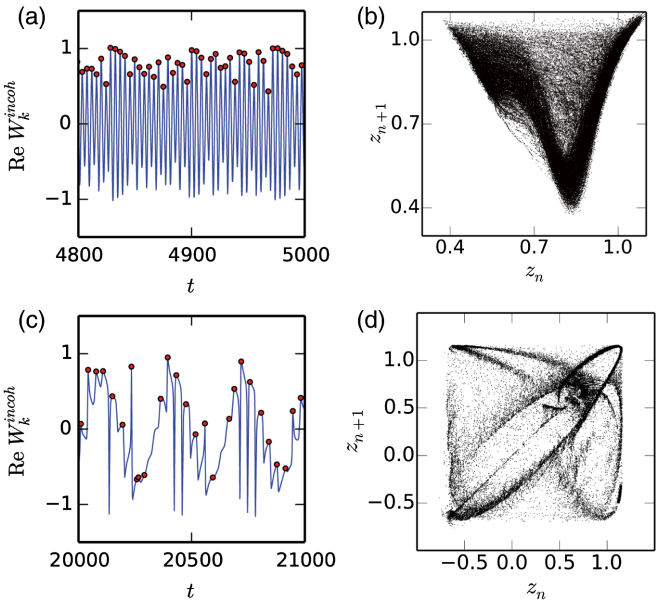

FIG. 3 (color online). Chaos in the chimera states. (a),(c) Samples of time series of incoherent oscillators for type I and II chimeras, respectively. Identified peaks are marked with circles. (b),(d) Next-maximum maps for the peaks in (a),(c).

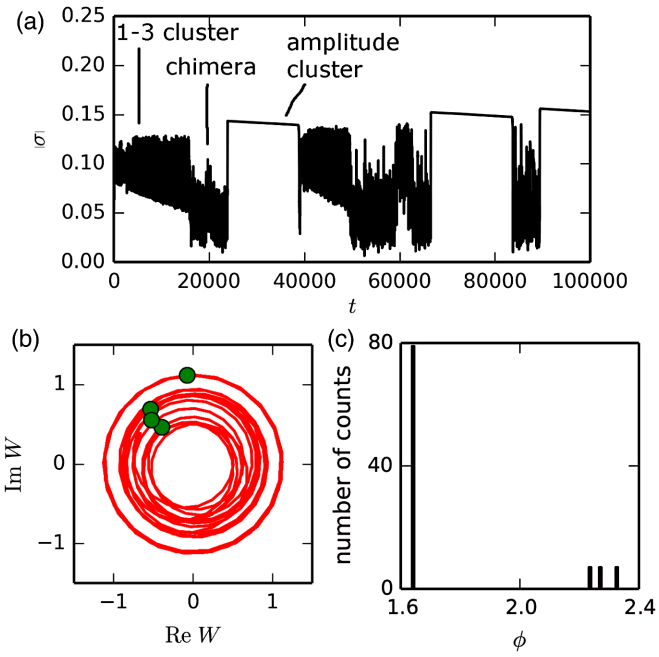

FIG. 4 (color online). Heteroclinic connections between type I chimeras, 1-3 cluster states and amplitude clusters for $N = 100$ oscillators. (a) Trajectory of $|\sigma|$ in time showing the transitions between the different states. (b) Exemplary dynamics of the 1-3 cluster state in the complex plane: lines depict time evolution and dots represent the configuration of the oscillators at one time step. (c) Histogram of phases in the 1-3 clusters state showing that it consists of 1 large cluster and 3 small clusters of approximately the same size.

define a measure characterizing the different dynamical states. The natural choice of the Kuramoto order parameter is inappropriate here, because of the strong amplitude fluctuations and since $\langle W\rangle = \eta \exp(-i\nu t)$ at all times. Therefore, we use the variance $\sigma = \langle W^2\rangle - \langle W\rangle^2$. An exemplary time series of $|\sigma|$ for parameters of type I chimeras is shown in Fig. 4(a).

Three qualitatively different regimes can be identified and after an initial transient, the system randomly settles first to one of them; in the trajectory shown, it is a 1-3 cluster state. The dynamics in this state are depicted in Fig. 4(b), and the phase distribution at one time step is shown in a histogram in Fig. 4(c). This state consists of one large cluster and three small clusters of approximately the same size. The measure $|\sigma|$ exhibits strong variations around a value of approximately 0.1. Then around $t = 15\,000$, the 1-3 cluster state breaks down and the system moves to a new state that exhibits fluctuations of $|\sigma|$ around 0.05: the type I chimera state. After approximately $\Delta t = 10\,000$, we observe another transition to a state with nearly constant $|\sigma|$. This is the amplitude cluster state as depicted in Fig. 1(a). Figure 4(a) suggests that transitions between these three states follow in a noncyclic and nonperiodic sequence. Thus, though being reminiscent of a heteroclinic orbit, the dynamics possesses a further peculiar, unpredictable feature.

In summary, we found numerically two types of chimera states in the vicinity of two types of clusters. The chimera states inherit properties from the respective cluster states. We conclude that the clustering mechanism is a first symmetry-breaking step sufficient for chimera states to occur in oscillatory systems with uniform global coupling. It differentiates the system into two groups, thereby rendering it bistable. Oscillators in the two states respond effectively different to the coupling due to nonlinear amplitude effects. Note that as a consequence, this mechanism will not give rise to chimeras in ensembles of phase oscillators, where other mechanisms may render their formation possible [11]. Furthermore, we demonstrated that the chimera states can mediate between cluster states and completely incoherent behavior as well as between cluster states and synchrony. This leads us to the conclusion that chimera states might appear spontaneously in many globally coupled systems, as a clustering mechanism and the possibility of amplitude variations are sufficient features a system has to exhibit.

We thank Vladimir García-Morales and Konrad Schönleber for fruitful discussions. Furthermore, we gratefully acknowledge financial support from the *Deutsche Forschungsgemeinschaft* (Grant No. KR1189/12-1), the *Institute for Advanced Study, Technische Universität München*, funded by the German Excellence Initiative, and the cluster of excellence *Nanosystems Initiative Munich (NIM)*.

*krischer@tum.de

[1] Y. Kuramoto and D. Battogtokh, Nonlinear Phenom. Complex Syst. **5**, 380 (2002).
[2] D. K. Umberger, C. Grebogi, E. Ott, and B. Afeyan, Phys. Rev. A **39**, 4835 (1989).
[3] K. Kaneko, Physica (Amsterdam) **41D**, 137 (1990).
[4] N. Nakagawa and Y. Kuramoto, Prog. Theor. Phys. **89**, 313 (1993).
[5] D. M. Abrams and S. H. Strogatz, Phys. Rev. Lett. **93**, 174102 (2004).
[6] S.-i. Shima and Y. Kuramoto, Phys. Rev. E **69**, 036213 (2004).
[7] D. M. Abrams, R. Mirollo, S. H. Strogatz, and D. A. Wiley, Phys. Rev. Lett. **101**, 084103 (2008).
[8] G. Bordyugov, A. Pikovsky, and M. Rosenblum, Phys. Rev. E **82**, 035205 (2010).
[9] C. R. Laing, Phys. Rev. E **81**, 066221 (2010).
[10] I. Omelchenko, Y. Maistrenko, P. Hövel, and E. Schöll, Phys. Rev. Lett. **106**, 234102 (2011).
[11] A. Yeldesbay, A. Pikovsky, and M. Rosenblum, Phys. Rev. Lett. **112**, 144103 (2014).
[12] G. C. Sethia and A. Sen, Phys. Rev. Lett. **112**, 144101 (2014).
[13] M. R. Tinsley, N. Simbarashe, and K. Showalter, Nat. Phys. **8**, 662 (2012).
[14] A. M. Hagerstrom, T. E. Murphy, R. Roy, P. Hövel, I. Omelchenko, and E. Schöll, Nat. Phys. **8**, 658 (2012).
[15] E. A. Martens, S. Thutupalli, A. Fourriére, and O. Hallatschek, Proc. Natl. Acad. Sci. U.S.A. **110**, 10563 (2013).
[16] S. Nkomo, M. R. Tinsley, and K. Showalter, Phys. Rev. Lett. **110**, 244102 (2013).
[17] M. Wickramasinghe and I. Z. Kiss, PLoS One **8**, e80586 (2013).
[18] L. Schmidt, K. Schönleber, K. Krischer, and V. García-Morales, Chaos **24**, 013102 (2014).
[19] M. J. Panaggio and D. M. Abrams, arXiv:1403.6204v2.
[20] C. R. Laing, Physica D (Amsterdam) **238**, 1569 (2009).
[21] O. E. Omel'chenko, Nonlinearity **26**, 2469 (2013).
[22] H. Daido and K. Nakanishi, Phys. Rev. Lett. **96**, 054101 (2006).
[23] H.-G. Purwins, H. U. Bödeker, and S. Amiranashvili, Adv. Phys. **59**, 485 (2010).
[24] K. Krischer, in *Advances in Electrochemical Science and Engineering* edited by R. C. Alkire and D. M. Kolb (Wiley-VCH, Weinheim, 2003), Vol. 8, p. 89.
[25] F. Mertens, R. Imbihl, and A. Mikhailov, J. Chem. Phys. **99**, 8668 (1993).
[26] F. Mertens, R. Imbihl, and A. Mikhailov, J. Chem. Phys. **101**, 9903 (1994).
[27] Y. Kuramoto, *Chemical Oscillations, Waves, and Turbulence* (Dover Publications, Inc., Mineola, New York, 2003).
[28] I. Miethe, V. García-Morales, and K. Krischer, Phys. Rev. Lett. **102**, 194101 (2009).
[29] V. García-Morales, A. Orlov, and K. Krischer, Phys. Rev. E **82**, 065202 (2010).
[30] L. Schmidt, K. Schönleber, V. García-Morales, and K. Krischer, arXiv:1405.0414.
[31] K. Schönleber, C. Zensen, A. Heinrich, and K. Krischer, New J. Phys. **16**, 063024 (2014).
[32] L. Schmidt and K. Krischer, Phys. Rev. E **90**, 042911 (2014).
[33] See Supplemental Material at http://link.aps.org/supplemental/10.1103/PhysRevLett.114.034101 for phase diagrams in the vicinity of the two types of chimera states.